

Dehydration-Rehydration Studies on Polytypes of Chloride and Nitrate Layered Double Hydroxides of Nordstrandite and Bayerite: a Comparative Study

Kavitha Venkataraman and Grace S. Thomas*



Cite This: *ACS Omega* 2022, 7, 5393–5400



Read Online

ACCESS |



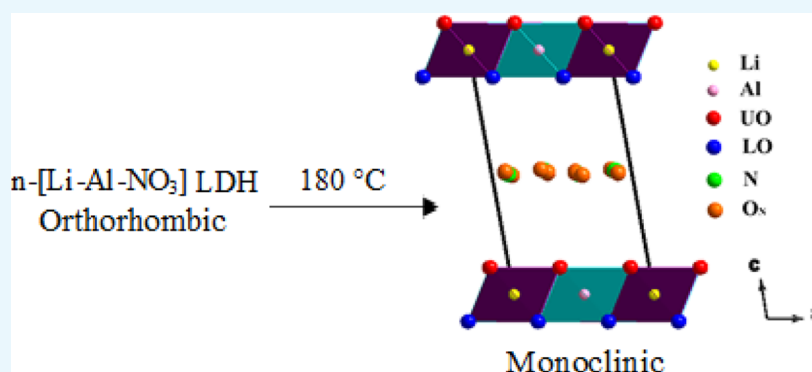
Metrics & More



Article Recommendations



Supporting Information



ABSTRACT: In this work, we report for the first time, the dehydration-rehydration studies of nordstrandite-derived layered double hydroxides (LDHs) of Li and Al, n -[Li–Al–X] ($X = \text{Cl}^-$ and NO_3^-) (n -nordstrandite derived). n -[Li–Al– NO_3], an orthorhombic phase, dehydrated at 180 °C to a monoclinic phase. Refinement placed the NO_3^- ions parallel to the hydroxide layers. The dehydration showed no change in basal spacing. The monoclinic n -[Li–Al–Cl] dehydrated at 160 °C with a 0.49 Å compression in basal spacing to an orthorhombic polytype. We compared our results with the published results of their bayerite counterparts b -[Li–Al–X] (b -bayerite derived) and observed that though n -[Li–Al–X] and b -[Li–Al–X] LDHs have similar structures, their dehydrated phases are structurally different. We also report the refinement of b -[Li–Al–Cl] (DH). Previous studies attribute the basal spacing values to the (i) degree of hydration and (ii) orientation of anions in the interlayer. We observe that basal spacing is a manifestation of the symmetry of the crystal. Dehydration of nitrate intercalated LDH, which proceeds from an orthorhombic symmetry to a monoclinic symmetry with no decrease in the interlayer spacing, is attributed to sliding of the hydroxyl layers in the ab -plane due to the increase in the β value. This sliding stabilizes the interlayer through weak long-range electrostatic forces that mainly contribute to the stabilization of the layered structure at separations much larger than the effective radius of hydrogen bonds. Such stabilization would negate the need for the layers to compress, thus conserving the basal spacing in n -[Li–Al– NO_3] (DH).

1. INTRODUCTION

Aluminum hydroxide, $\text{Al}(\text{OH})_3$, possesses a layered structure consisting of hydroxyl layers. Two-thirds of the octahedral sites are occupied by Al^{3+} ions, and the remaining one-third are vacant resulting in charge-neutral hydroxyl layers of composition $[\text{Al}_{2/3}\square_{1/3}(\text{OH})_2]$ (\square : cation vacancy). The four polymorphic modifications of $\text{Al}(\text{OH})_3$ are gibbsite,^{1,2} bayerite,³ nordstrandite,^{4–7} and doyleite.⁸ These polymorphs with vacant cation sites tend to take up Li^+ ions to form layered double hydroxides (LDHs) of Li and Al through an imbibition reaction with saturated solutions of LiX salts. These insertion reactions are kinetically unfavorable, and the high activation energy required for the reaction is provided by hydrothermal treatment of the samples resulting in the thermodynamically stable phase. Li^+ ions incorporate into the cation vacancies of $\text{Al}(\text{OH})_3$ and anions, with their hydration spheres into the interlayer gallery to

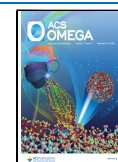
yield a composition $[\text{Li}_{1/3}\text{Al}_{2/3}(\text{OH})_2] [\text{A}^{n-}]_{1/3m} \cdot x\text{H}_2\text{O}$ ($\text{A} = \text{Cl}^-, \text{Br}^-, \text{CO}_3^{2-}, \text{NO}_3^-, \text{SO}_4^{2-}, \text{and } \text{ClO}_4^-$). The $[\text{Li}_{1/3}\text{Al}_{2/3}(\text{OH})_2]^{1/3+}$ layer group symmetry is reported to be $P\bar{3}12/m$ with the threefold axis perpendicular to the layer and the twofold axis parallel to the layer.⁹

In LDHs, the bonding within the metal hydroxide layer is strong ionic-covalent while it is weak van der Waals forces between the consecutive layers. The weak bonding between metal hydroxide layers allows the layers to be stacked in

Received: November 23, 2021

Accepted: January 25, 2022

Published: February 3, 2022



numerous ways to get a variety of polytypes, and this phenomenon is known as polytypism. In general, the molecular symmetry of an interlayer anion plays a vital role in governing the choice of the polytype, and the variation in the degree of hydration leads to different polytypic transformations. Small anions with high charge density are strongly attracted to the positive end of the water molecules leading to higher hydration enthalpies.¹⁰ A sulfate anion will intercalate with its large hydration sphere, and hence the basal spacing of SO_4^{2-} -intercalated LDHs is larger compared to Cl^- , Br^- , NO_3^- , and ClO_4^- intercalated LDHs.¹¹ Upon heating, LDHs lose their intercalated water with a consequent compression in the interlayer spacing and could transform into different polytype structures. The water molecules in the interlayer are exchangeable with ambient humidity, and hence these transformations are reversible. Polytype selectivity in [Li–Al] LDHs is influenced by the layer stacking in the $\text{Al}(\text{OH})_3$ polymorphic precursor used for the synthesis. Gibbsite has a $\overline{P}\overline{P}\overline{P}$ stacking sequence, where the metal hydroxide layer is represented by the symbol P , and \overline{P} is the mirror image of P .¹² In the gibbsite-derived LDHs, g -[Li–Al–X] LDHs ($X = \text{Cl}^-$, Br^- , NO_3^- , SO_4^{2-} , and ClO_4^-) (g -gibbsite derived), the metal hydroxide layers are stacked exactly one above the other without any translation in such a way that the threefold axis normal to the layer is conserved yielding a two-layer hexagonal structure (2H). Bayerite on the other hand has $\overline{P}\overline{P}\overline{P}$ stacking.³ In bayerite-derived LDHs, b -[Li–Al–X] LDHs ($X = \text{Cl}^-$, Br^- , NO_3^- , SO_4^{2-} , and ClO_4^-) (b -bayerite derived), the metal hydroxide layers are translated either along a - or b -crystallographic axis, thereby eliminating the coincidence of the threefold axis along the stacking direction, yielding a one-layer monoclinic structure (1 M).

The polytypic transformations and basal spacing dynamics of both gibbsite- and bayerite-derived LDHs on dehydration and rehydration are well studied. The g -[Li–Al–X] LDHs ($X = \text{Cl}^-$, Br^- , NO_3^- , SO_4^{2-} , and ClO_4^-) are reported to retain their two-layered hexagonal structure at different degrees of hydration.^{13–16} The b -[Li–Al–X] LDHs on the other hand may retain their one-layer hexagonal structure or transform to a one-layer monoclinic structure depending on the anion present in the interlayer and the degree of hydration.^{10,11,16–18} However, the dehydration-rehydration behavior of nordstrandite-derived LDHs has not been explored till date.

Nordstrandite has a one-layer structure of triclinic crystal symmetry.^{7,19} In our earlier work on the synthesis of n -[Li–Al–X] LDHs (n -nordstrandite derived, $A = \text{Cl}^-$ and NO_3^-), we observed that the powder X-ray diffraction (PXRD) patterns of n -[Li–Al–X] LDHs were identical to those of their bayerite-derived counterparts at ambient humidity.²⁰ Interestingly, even though both b -[Li–Al–Cl] and n -[Li–Al–Cl] have a one-layer monoclinic structure, they differ in the position of anions and water molecules in the interlayer.²⁰ Consequently, we ask the following questions.

- Will there be any remarkable difference in the dehydration-rehydration behavior of n -[Li–Al–A] as opposed to b -[Li–Al–A] LDHs?
- Will the dehydrated phases of n - and b -derived LDHs be structurally different?

To answer the aforementioned questions, we performed the dehydration/rehydration studies on n -[Li–Al–A] LDHs ($A = \text{Cl}^-$ and NO_3^-) and compared our observations with the reported behavior of their bayerite counterparts.

2. RESULTS

2.1. n -[Li–Al–NO₃]. The PXRD pattern of n -[Li–Al–NO₃] comprises two basal reflections at 2θ 9.9 and 19.8° and numerous sharp and less intense reflections in the 2θ range 12–17° and 25–35°, a pattern similar to that of b -[Li–Al–NO₃] (Figure S1). Previously, Nagendran et al. in their extensive study of the structure of b -[Li–Al–NO₃] indexed the pattern to a cell of orthorhombic symmetry. n -[Li–Al–NO₃] LDH could also be indexed to a cell of orthorhombic symmetry.¹⁸ In both cases, the structure of the as-prepared phases could not be refined because of nonavailability of a model.

The synthesized n -[Li–Al–NO₃] is stoichiometric with $[\text{Li}^+]/[\text{Al}^{3+}] = 0.48$ and $[\text{Li}^+]/[\text{NO}_3^-] = 0.97$. Thermogravimetric analysis (TGA) showed the three-step mass loss of a typical LDH material. The first-step mass loss was 15.82%. The mass of the final residue was 41.41% which was attributed to $\text{LiAlO}_2 + 0.5\text{Al}_2\text{O}_3$ (Figure S2a). Hence, the empirical formula corresponds to $[\text{Li}_{0.39}\text{Al}_{0.81}(\text{OH})_3(\text{NO}_3)_{0.40}\cdot 1.15\text{H}_2\text{O}]$. Compositional analysis is given in Table S1.

2.2. Hydration Studies on n -[Li–Al–NO₃]. n -[Li–Al–NO₃] was heated to obtain a completely dehydrated phase at 180 °C. This phase is henceforth represented as n -[Li–Al–NO₃] (DH). The pattern was indexed to a one-layer cell of monoclinic symmetry with the cell parameters $a = 5.0962$ Å, $b = 8.8253$ Å, $c = 9.0943$ Å, and $\beta = 100.76^\circ$ (Table 1).²¹ When the

Table 1. Observed 2θ Values [°] and the corresponding hkl Indices of n -[Li–Al–NO₃] (DH)^a

n -[Li–Al–NO ₃] (DH)	
$a = 5.0962$ Å, $b = 8.8253$ Å, $c = 9.0943$ Å, $\alpha = \gamma = 90.0^\circ$ $\beta = 100.76^\circ$	
FM value = 22.79, De Wolff's Mn value = 44.89	
2θ [°]	hkl
9.9	001
19.8	002
35.88	–131
37.77	131
39.18	–212
40.38	004
44.68	–133
51.92	203
57.5	134
60.55	–243
63.21	–331
64.16	–330
66.86	–324
74.87	–260
76.93	410
80.49	–172

^aObtained using the code APPLEMAN, part of the PROZKI suite of programs.²¹

sample was cooled and rehydrated, we got back the pattern of the as-prepared phase. In order to simulate the PXRD pattern of n -[Li–Al–NO₃] (DH), we used code DIFFaX.^{22,23} The stacking of metal hydroxide layers using the stacking vector $(1/3, 0, z)$ yielded a pattern matching with the experimental pattern (Figure 1).²⁴ This corresponds to a monoclinic structure of the $C12_1/m1$ space group. Further this structure was used as a partial structure model for refinement of n -[Li–Al–NO₃] (DH). A baffling observation was that the dehydration took place without any change in the basal spacing (Figure S3).

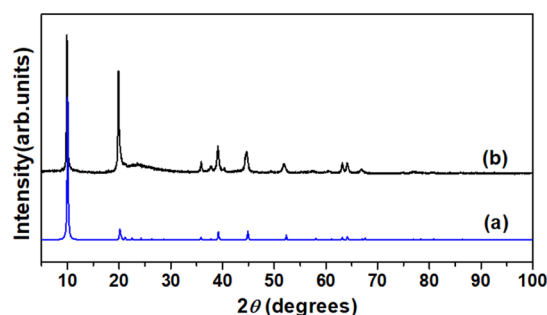


Figure 1. PXRD patterns of n -[Li–Al–NO₃] (DH). (a) DIFFaX simulated and (b) experimental.

2.3. Structure Determination of n -[Li–Al–NO₃] (DH). A le Bail fit was performed in the space group $C12_1/m1$ using the code FOX.²⁵ The R_{wp} and R_p values obtained were 0.1190 and 0.0991, respectively. The structure model of n -[Li–Al–Cl] reported in our earlier work was used, and the layer for $C12_1/m1$ was introduced.²⁰ Nitrate ion was introduced into the interlayer and allowed to move freely. A Monte Carlo approach was used to locate the position of the nitrate ion in the interlayer. In order to eliminate improbable crystallographic positions, we fixed the position of the nitrate ion midway between the hydroxyl layers ($z = 0.5$) and refined its position along x - and y - axes. The occupancy of the nitrate ion was also fixed as 0.25 to preserve the calculated value. The nitrate ion took up the $8j$ position parallel to the metal hydroxide layers. The R_{wp} and R_p values were 0.1750 and 0.1617, respectively. In order to complete the refinement, the model was taken to FULLPROF suite.^{26,27} The R_{wp} and R_p values after final refinement were 0.1480 and 0.1150. The Rietveld fit and the refined structure are given in Figures 2 and 3, and the refined parameters and atomic coordinates are given in Tables 2 and 3. The refined bond distances and angles are given in Table S2.

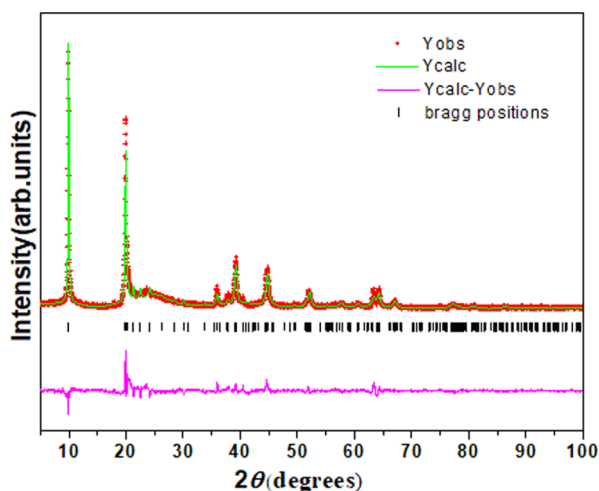


Figure 2. Rietveld fit of the PXRD pattern of n -[Li–Al–NO₃] (DH).

The scanning electron microscopy (SEM) micrographs of the as-prepared LDHs from both bayerite and nordstrandite exhibit similar platelet features. Thus, the morphology does not throw any light on the difference in the crystal structure of the dehydrated phases (Figure S4).

To summarize, Nagendran et al. have reported a one-layer hexagonal phase at 150 °C on dehydration of b -[Li–Al–NO₃]

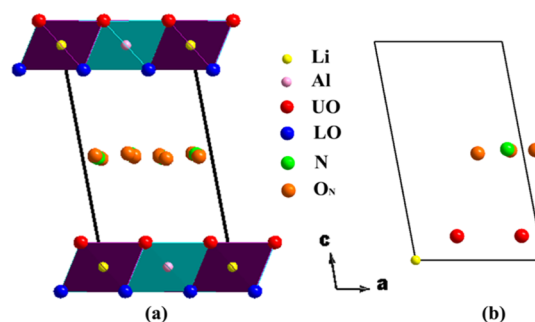


Figure 3. Refined structure of n -[Li–Al–NO₃] (DH) viewed (a) along the b -crystallographic axis and (b) asymmetric unit.

Table 2. Results of Rietveld Refinement of n -[Li–Al–NO₃] (DH) and b -[Li–Al–Cl] (DH)

	n -[Li–Al–NO ₃] (DH)	b -[Li–Al–Cl] (DH)
molecular formula	[Li ₂ Al ₄ (OH) ₁₂](NO ₃) ₂	[Li ₂ Al ₄ (OH) ₁₂]Cl ₂
crystal system	monoclinic	hexagonal
space group	$C12_1/m1$	$P\bar{3}1m$
a (Å)	5.0877(16)	5.1098(2)
b (Å)	8.8140(3)	5.1098(2)
c (Å)	9.0504(10)	7.1704(3)
α (°)	90	90
β (°)	100.51(3)	90
γ (°)	90	120
volume (Å ³)	399.04(18)	162.139(13)
parameters refined	15	17
R_{wp}	14.8	16.4
R_p	11.5	12.3
$R(F^2)$	4.86	4.24
χ^2	3.42	2.57

Table 3. Refined Atomic Coordinates of n -[Li–Al–NO₃] (DH) and b -[Li–Al–Cl] (DH)

atom	wyckoff position	x	y	z	occupancy
n -[Li–Al–NO ₃] (DH)					
Li	2a	0	0	0	1
Al	4g	0	0.33130	0	1
O1	8j	0.86631	0.16980	0.11097	1
O2	4i	0.35940	0	0.10970	1
N	8j	0.88176	0.13769	0.50744	1
O3	8j	0.64369	0.08427	0.48833	1
O4	8j	1.09983	0.05632	0.50296	1
O5	8j	0.90177	0.28479	0.50127	1
b -[Li–Al–Cl] (DH)					
Li	1a	0	0	0	1
Al	2c	0.33330	0.66670	0	1
O1	6k	0	0.63615	0.13340	1
Cl	1b	0	0	0.5	1

with a ~ 1.7 Å decrease in basal spacing.¹⁸ We report a monoclinic phase on dehydration of n -[Li–Al–NO₃] at 180 °C with no change in basal spacing. Refinement of the dehydrated phase places the nitrate ions parallel to the hydroxyl layers.

2.4. Dehydration-Rehydration Studies on n -[Li–Al–Cl]. In our previous work, we have refined n -[Li–Al–Cl] to a monoclinic structure²⁰ and reported that the as-prepared phases of both n and b -[Li–Al–Cl] have similar PXRD patterns. We report here the results of the dehydration-rehydration study on n -[Li–Al–Cl] and compare them with the behavior of b -[Li–

Al–Cl] reported by Britto and Kamath.²⁸ The compositional analyses of both b-[Li–Al–Cl] and n-[Li–Al–Cl] are given in Table S1.

The complete dehydration of n-[Li–Al–Cl] happened at 160 °C with 0.49 Å compression in the basal spacing. The dehydrated sample is designated as n-[Li–Al–Cl] (DH). In contrast, the dehydration of b-[Li–Al–Cl] happened at a significantly lower temperature of 125 °C though with a similar decrease in basal spacing (Figure S5). The dehydrated bayerite-derived sample will henceforth be referred to as b-[Li–Al–Cl] (DH). The PXRD patterns of both the dehydrated samples look similar, except for three additional reflections in n-[Li–Al–Cl] (DH) at 2θ 29.98, 34.69, and 49.90° (Figure 4). When the n-

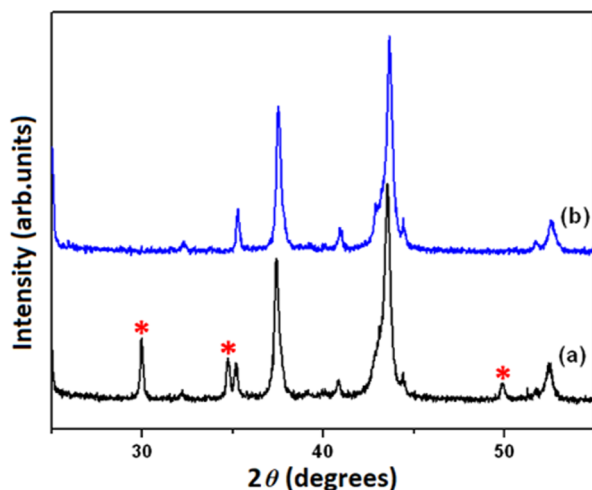


Figure 4. Mid 2θ region of PXRD patterns of (a) n-[Li–Al–Cl] (DH) and (b) b-[Li–Al–Cl] (DH). The additional peaks of n-[Li–Al–Cl] (DH) are marked with an asterisk.

[Li–Al–Cl] (DH) sample was cooled and rehydrated, we obtained the ambient pattern. On repeating the dehydration, the extra reflections persisted. This confirmed that the polytype obtained on dehydration of n-[Li–Al–Cl] is structurally different from that obtained from b-[Li–Al–Cl].

Attempts to simulate the PXRD pattern of n-[Li–Al–Cl] (DH) using DIFFaX did not yield a satisfactory fit. Code POWDER, a part of PROZKI suite of programs, was then invoked without imposing any symmetry restraints. A series of cell parameters were generated, all of which pointed to a cell of orthorhombic symmetry. Among the possible solutions, the set, in closest agreement with the cell parameters obtained from the PXRD pattern, was selected. The cell parameters so obtained were $a = 5.3359$ Å, $b = 8.8466$ Å, $c = 14.3261$ Å, and $\alpha = \beta = \gamma = 90.0^\circ$. However, we were unsuccessful in indexing the pattern using these cell parameters.

2.5. Structure Refinement of b-[Li–Al–Cl] (DH). Britto et al. have reported the dehydration studies of b-[Li–Al–Cl]; however, the structural refinement of the dehydration product was not done. The PXRD pattern of b-[Li–Al–Cl] (DH) was indexed to a one-layer cell of hexagonal symmetry with the cell parameters $a = b = 5.09669$ Å and $c = 7.13335$ Å (Table 4). Using code DIFFaX, the layer relationship in b-[Li–Al–Cl] (DH) was simulated using the (0, 0, 1) stacking vector.²⁴ The simulated PXRD was a good match with the experimental pattern that was reported earlier by Britto and Kamath (Figure 5).²⁸

Table 4. Observed 2θ Values [°] and the Corresponding hkl Indices of b-[Li–Al–Cl] (DH)^a

b-[Li–Al–Cl] (DH)	
$a = b = 5.09669$ Å, $c = 7.13335$ Å, $\alpha = \beta = 90.0^\circ$ $\gamma = 120.0^\circ$	
FM value = 51.11, De Wolff's Mn value = 87.94	
2θ [°]	hkl
12.47	001
23.78	101
25	002
32.3	102
35.24	110
37.55	111
40.92	200
42.89	201
43.66	112
52.63	113
56.64	211
61.32	212
63.22	300
63.69	114
64.67	301
69.05	302
74.41	220
75.83	221
79.36	311
79.96	222
89.76	223
90.18	313
91.33	116
96.12	224

^aObtained using the code APPLEMAN, part of the PROZKI suite of programs.²¹

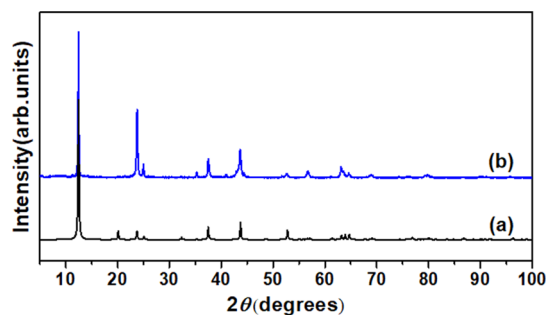


Figure 5. PXRD patterns of b-[Li–Al–Cl] (DH). (a) DIFFaX simulated and (b) experimental.

We attempted the structure refinement by doing a Le Bail fit with $P\bar{3}1m$ space group in the code FOX.²⁵ At this stage, $R_{wp} = 0.1592$ and $R_p = 0.0842$. The metal hydroxide layer from a reported dehydrated b-[Li–Al–Br] LDH was used as a partial structure model.²⁴ The chloride ion was introduced in the interlayer and was allowed to translate freely in the interlayer. The position and occupancy of the chloride ion were refined. A Monte Carlo procedure was used, and each time, the computed and experimental patterns were compared. A decent fit was observed between the computed and experimental patterns when the chloride ion took up a special position $1b$, which is located midway between the hydroxyl layers. The R_{wp} and R_p values were 0.219 and 0.156. The refinement performed in FOX was in direct space. In order to complete the refinement in the reciprocal space, the above model was imported to FULLPROF

suite.^{26,27} The Rietveld fit and the final refined structure are given in Figures 6 and 7. The final R_{wp} and R_p values were 0.164

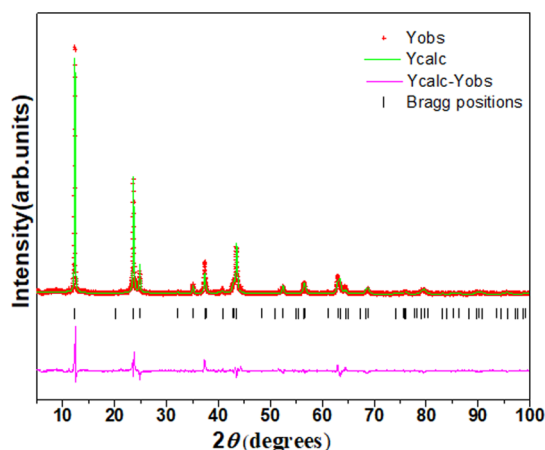


Figure 6. Rietveld fit of the PXRD pattern of b-[Li-Al-Cl] (DH).

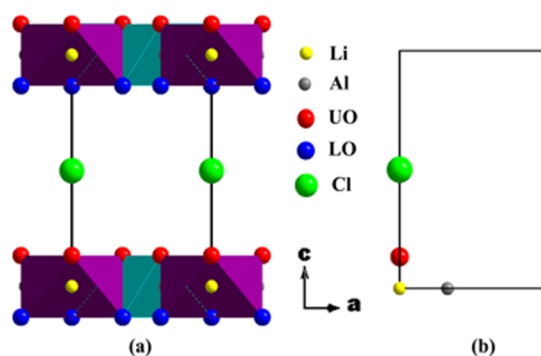


Figure 7. Refined structure of b-[Li-Al-Cl] (DH) viewed (a) along the *b*-crystallographic axis and (b) asymmetric unit.

and 0.123. The R_{Bragg} value is 7.35 which is in the acceptable range for the goodness of fit. The results of refined parameters and atomic coordinates are given in Tables 2 and 3. The refined bond lengths and angles are given in Table S2.

3. DISCUSSION

Venkatraman and Pachyappan report that though bayerite is monoclinic and nordstrandite is triclinic, both yield [Li-Al-X] LDHs, X = Cl⁻, Br⁻, NO₃⁻, and SO₄²⁻ with similar powder patterns and morphology and therefore appear to have similar crystal structures.²⁰ They further report that it is the local symmetry C1 in the interlayer region of nordstrandite that renders the interlayer gallery unsuitable for the accommodation of the anions. The intercalating anions along with the water molecules mediate a layer translation through H-bonding in nordstrandite, yielding n-[Li-Al-X] LDHs whose structures are identical to those of their bayerite counterparts. However, dehydration-rehydration studies carried out in this work show significant differences in the behavior of n-[Li-Al-X], X = Cl⁻ and NO₃⁻ as opposed to their bayerite counterparts in terms of their (i) dehydration temperatures and (ii) symmetries of the dehydrated products (Table 5).

The higher dehydration temperatures of the n-[Li-Al] LDHs can be attributed to stronger hydrogen bonding and a higher water content. In b-[Li-Al-Cl], the Cl⁻ ion is reported to be weakly hydrogen bonded to the water molecules in contrast to n-

Table 5. Dehydration Behavior of n,b-[Li-Al-X] LDHs where X = Cl⁻ and NO₃⁻

sample name	symmetry of as prepared phase	dehydration temperature (°C)	symmetry of dehydrate
n-[Li-Al-Cl]	monoclinic	160	orthorhombic
b-[Li-Al-Cl]	monoclinic	125	hexagonal
n-[Li-Al-NO ₃]	orthorhombic	180	monoclinic
b-[Li-Al-NO ₃]	orthorhombic	150	hexagonal

[Li-Al-Cl] LDH, where the Cl⁻ ions are strongly hydrogen bonded with the water molecules.^{17,20} Moreover, TGA results show an 18.6% weight loss for the nordstrandite-derived sample as compared to a 8.7% weight loss for the bayerite-derived sample, which suggest the presence of extensive H-bonding in the nordstrandite-derived sample compared to the bayerite counterpart (Table S1). The higher dehydration temperature of the n-[Li-Al-NO₃] LDHs is indicative of stronger hydrogen bonding between the anion and the interlayer water molecules. TGA results show a 15.8% weight loss in n-[Li-Al-NO₃] LDH versus 8.4% for b-[Li-Al-NO₃] LDH. Polyatomic anions like NO₃⁻ with multiple oxygens are expected to have a greater extent of hydrogen bonding with layer hydroxyls as compared to a monovalent anion such as Cl⁻, which would account for the 20° higher dehydration temperature of n-[Li-Al-NO₃] as compared to b-[Li-Al-NO₃].

The loss of water during the transformation of the as-prepared LDH appears to have a remarkable effect on the symmetry of the final dehydrated phase. Dehydration of both orthorhombic b-[Li-Al-NO₃] and monoclinic b-[Li-Al-Cl] as well as monoclinic n-[Li-Al-Cl] led to the formation of higher symmetry dehydrated polytypes (Table 5). In contrast, orthorhombic n-[Li-Al-NO₃] is the only precursor which yielded a lower symmetry monoclinic dehydrate. Further, this change took place with no decrease in basal spacing. Intuitively, we expect a decrease in basal spacing on dehydration of an LDH. Nagendran et al. have reported that both g and b-[Li-Al-NO₃] followed this trend and showed a decrease in the basal spacing of ~1.7 Å on dehydration.^{13,18} They relate the decreased basal spacing to the orientation of the anion in the interlayer region. Interestingly, there are also some reports of NO₃⁻ intercalated LDHs such as g-[Zn-Al₄-NO₃] that show no significant difference in basal spacing on dehydration.^{29,30}

To study the relationship between the symmetry of the dehydrated phase and the change in basal spacing, basic crystallographic formulae were used to calculate the “*d*” spacing in the stacking direction (Table S3). In LDHs, the stacking of the hydroxyl layers is along the 00*l* direction. The *d* spacing was calculated for n-[Li-Al-NO₃], b-[Li-Al-NO₃], g-[Li-Al-NO₃], and g-[Zn-Al₄-NO₃], and the values so obtained are compared with the experimental values in Table 6. Any change from orthorhombic to hexagonal symmetry proceeds with an increase in the γ value while conserving the “*c*” axes as the stacking direction as well as the principal axes. Consequently, dehydration involving such a transformation is accompanied by a decrease in both the “*c*” parameter and “*d*” spacing to the same extent as seen in dehydrated g- and b-[Li-Al-NO₃] LDHs that show compression of basal spacing by 1.7 Å (Table 6). However, change in symmetry from orthorhombic to monoclinic on dehydration in n-[Li-Al-NO₃] proceeds with an increase in the β value accompanied by sliding of the layers in the *ab*-plane. Such sliding of layers kicks in the weak long-range electrostatic interlayer forces that mainly contribute to the stabilization of the

Table 6. Observed and Calculated *d*-Spacing for the Nitrate Intercalated LDHs

		as prepared	dehydrated
n-[Li-Al-NO ₃] (in this work)	symmetry	orthorhombic	monoclinic
	cell parameters	$a = 11.72 \text{ \AA}, b = 9.51 \text{ \AA}, c = 8.96 \text{ \AA}$ (indexed)	$a = 5.0878 \text{ \AA}, b = 8.8138 \text{ \AA}, c = 9.0515 \text{ \AA}, \beta = 100.49^\circ$ (refined)
	<i>d</i> -spacing observed (\AA)	8.93	8.93
	^a <i>d</i> -spacing calculated (\AA)	8.93	8.9
	difference in <i>d</i> -spacing	nil	
b-[Li-Al-NO ₃] ¹⁸ (reported)	symmetry	orthorhombic	hexagonal
	cell parameters	$a = 11.72 \text{ \AA}, b = 9.51 \text{ \AA}, c = 8.96 \text{ \AA}$ (indexed)	$a = 5.1217 \text{ \AA}, c = 7.2833 \text{ \AA}$ (refined)
	<i>d</i> -spacing observed (\AA)	8.95	7.26
	^a <i>d</i> -spacing calculated (\AA)	8.95	7.28
	difference in <i>d</i> -spacing	$\sim 1.7 \text{ \AA}$	
g-[Li-Al-NO ₃] ¹³ (reported)	symmetry	orthorhombic	hexagonal
	cell parameters	$a = 12.5 \text{ \AA}, b = 15.72 \text{ \AA}, c = 17.88 \text{ \AA}$ (indexed)	$a = 5.1252 \text{ \AA}, c = 14.4462 \text{ \AA}$ (refined)
	<i>d</i> -spacing observed (\AA)	8.92	7.2
	^a <i>d</i> -spacing calculated (\AA)	8.94	7.22
	difference in <i>d</i> -spacing	$\sim 1.7 \text{ \AA}$	
g-[Zn-Al ₄ -NO ₃] ²⁹ (reported)	symmetry	monoclinic	orthorhombic
	cell parameters	$a = 10.257 \text{ \AA}, b = 8.8626 \text{ \AA}, c = 17.2888 \text{ \AA}, \beta = 95.2^\circ$ (refined)	$a = 5.16 \text{ \AA}, b = 8.97 \text{ \AA}, c = 16.56 \text{ \AA}$ (indexed)
	<i>d</i> -spacing observed (\AA)	8.6	8.3
	^a <i>d</i> -spacing calculated (\AA)	8.6	8.3
	difference in <i>d</i> -spacing	$\sim 0.3 \text{ \AA}$	

^a*d*-Spacing values are calculated using crystallographic formulae for interplanar spacings, taken from appendix 1. Basic crystallography, practical electron microscopy. Note: The dehydrated phases of g-, b-, and n-[Li-Al-NO₃] have all been refined, and the as-prepared phases, though not refined, have been completely indexed.

layered structure at separations much larger than the effective radius of hydrogen bonds.³¹ Such a stabilization would negate the need for the layers to compress, thus conserving the basal spacing in n-[Li-Al-NO₃] (DH).

4. CONCLUSIONS

The as-prepared samples of nordstrandite-derived nitrate and chloride LDHs are similar to their bayerite counterparts. Despite this similarity, their respective dehydrated phases are structurally different. The dehydration of n-[Li-Al-NO₃] yielded a monoclinic polytype, whereas b-[Li-Al-NO₃] LDH gave a hexagonal polytype. n-[Li-Al-Cl] (DH) is orthorhombic, whereas b-[Li-Al-Cl] (DH) is a hexagonal polytype. An orthorhombic to hexagonal transformation of an LDH having interlayer nitrate anions will be accompanied by a decrease in the interlayer spacing. In contrast, a transformation from orthorhombic to monoclinic or vice versa will proceed with no change in basal spacing. In the absence of a complete structural refinement of hydrated and dehydrated phases, this general guideline can prove useful. Long-range electrostatic interlayer forces too play a critical role in the polytype selection and transformations in [Li-Al] LDHs.

5. EXPERIMENTAL SECTION

5.1. Synthesis. Nordstrandite was synthesized by following the Taichi's procedure.³² Al(OH)₃ was prepared in the form of a

gel by the addition of 25% NH₃ to 0.25 M AlCl₃ solution at the rate of 5 mL min⁻¹ at 25 °C until the pH reached to 8. The gel was washed with deionized water and aged in 8% ethylene diamine solution at 40 °C for 40 h. 0.5 g of nordstrandite was soaked in 10 mL of saturated LiX, (X = Cl⁻ and NO₃⁻) solution. The solution was treated hydrothermally in a Teflon-lined autoclave of capacity 80 mL to a temperature range of 110–140 °C for 24 h. The samples obtained after hydrothermal treatment were washed with Type II water (specific resistance 15 MΩ cm, Millipore Academic water purification system) and dried in a hot air oven at 60 °C.

For comparative study, the b-[Li-Al-X] (X = Cl⁻ and NO₃⁻) LDHs were synthesized according to the procedure reported by Britto and Kamath.¹⁷

5.2. Characterization. For sample characterization, the PXRD patterns were recorded using a Bruker D8 ADVANCE diffractometer (Cu Kα radiation, Ni filter, $\lambda = 1.5418 \text{ \AA}$) operating in reflection geometry (40 kV and 30 mA). The dehydration-rehydration studies were carried out within the diffractometer as an in situ measurement using an Anton Paar CHC plus Humidity Chamber as an attachment over the temperature range 30–180 °C. The sample was cooled to room temperature and allowed to rehydrate at ambient humidity, and its PXRD pattern was recorded again. For refinement, the PXRD patterns were recorded over a 5–100° 2θ range with a step size of 0.02° and a time step of 10 s step⁻¹. Indexing of the PXRD

patterns was carried out using the code APPELMAN, part of PROZKI suite of programs,²¹ and the refined cell parameters were obtained. The intercalated water content was estimated with the help of TGA over a temperature range of 30–900 °C at a heating rate 5 °C min⁻¹ in N₂ atmosphere using a Mettler Toledo TG (SDTA) model 851e system driven by STARe 7.01 software. Wet chemical analyses were performed to estimate the cations and anions. Li⁺ was estimated by flame photometry, Al³⁺ by gravimetry, and anions by ion chromatography (Metrohm model 861 advanced compact ion chromatograph fitted to a Metrosep SUP5 150 column). The IR spectra of the samples were recorded using a Bruker Alpha-P IR spectrometer (diamond attenuated total reflectance cell, 400–4000, 4 cm⁻¹ resolution). To understand the layer relationship in LDHs, the Fortran-based computer code DIFFaX is used.^{22,23} Within the DIFFaX formalism, a single metal hydroxide layer structure is taken from the reported structure, and all symmetry related atoms were fed into the input file. In order to broaden the Bragg reflections in the simulated patterns, a Lorentzian profile function with full width at half-maximum = 0.2° 2θ was given in the input file. Code DIFFaX computes the Laue symmetry when proclaimed UNKNOWN. It integrates the intensity obtained from a single layer and calculates it for infinite layers. By trial and error, different stacking vectors are used till we get a good agreement between the experimental and simulated patterns. This polytype structure is considered as the partial structure model, and the position of the metal hydroxide layer is used as such for refinement. For DIFFaX simulations, we used the reported structure of b-[Li-Al-Br] with the space group P $\bar{3}$ 1m as the starting structure.²⁴ Using code FOX, we identified the position and orientation of the intercalated anions.²⁵

Crystallographic data for this paper for n-[Li-Al-NO₃] (DH) and b-[Li-Al-Cl] (DH) (CCDC-2102212 and CCDC-2102213, respectively) have been uploaded to The Cambridge Crystallographic Data Centre via www.ccdc.cam.ac.uk/data_request/cif.

■ ASSOCIATED CONTENT

SI Supporting Information

The Supporting Information is available free of charge at <https://pubs.acs.org/doi/10.1021/acsomega.1c06630>.

PXRD patterns of n-[Li-Al-NO₃] and b-[Li-Al-NO₃], TGA plots of nordstrandite-derived LDHs, PXRD pattern of n-[Li-Al-NO₃] (DH), SEM micrographs of nordstrandite and nordstrandite- and bayerite-derived LDHs, PXRD patterns of n-[Li-Al-Cl] (DH) and b-[Li-Al-Cl] (DH), compositional analysis of LDHs, refined bond lengths and bond angles of n-[Li-Al-NO₃] (DH) and b-[Li-Al-Cl] (DH), and crystallographic formulas for interplanar spacings (PDF)

Crystallographic data for n-[Li-Al-NO₃] (DH) (CIF)

Crystallographic data for b-[Li-Al-Cl] (DH) (CIF)

■ AUTHOR INFORMATION

Corresponding Author

Grace S. Thomas – Department of Chemistry, Jyoti Nivas College, Bangalore 560 095, India; orcid.org/0000-0002-1712-4320; Email: gracesaraht@gmail.com

Author

Kavitha Venkataraman – Department of Chemistry, Jyoti Nivas College, Bangalore 560 095, India

Complete contact information is available at: <https://pubs.acs.org/doi/10.1021/acsomega.1c06630>

Notes

The authors declare no competing financial interest.

■ ACKNOWLEDGMENTS

K.V. thanks P. Vishnu Kamath and the group for all suggestions and discussions. K.V. thanks IISc Bangalore and DST-SAIF Cochin for the SEM micrographs.

■ REFERENCES

- (1) Megaw, H. D. The Crystal Structure of Hydrargillite, Al(OH)₃. *Z. für Kristallogr.—Cryst. Mater.* **1934**, *87*, 185–205.
- (2) Zhang, X.; Zhang, X.; Graham, T. R.; Pearce, C. I.; Mehdi, B. L.; N'Diaye, A. T.; Kerisit, S.; Browning, N. D.; Clark, S. B.; Rosso, K. M. Fast Synthesis of Gibbsite Nanoplates and Process Optimization Using Box-Behnken Experimental Design. *Cryst. Growth Des.* **2017**, *17*, 6801–6808.
- (3) Rothbauer, R.; Zigan, F.; O'Daniel, H. Refinement of the Structure of the Bayerite, Al(OH)₃ Including a Proposal for the h-Position. *Z. Kristallogr. N. Cryst. Struct.* **1967**, *125*, 317–331.
- (4) Saalfeld, H.; Mehrotra, B. B. To the Structure of Nordstrandite Al(OH)₃. *Naturwiss.* **1966**, *53*, 128–129.
- (5) Van Nordstrand, R. A.; Hettinger, W. P.; Keith, C. D. A New Alumina Trihydrate [17]. *Nature* **1956**, *177*, 713–714.
- (6) Violante, P.; Violante, A.; Tait, J. M. Morphology of Nordstrandite. *Clays Clay Miner.* **1982**, *30*, 431–437.
- (7) Bosmans, H. J. Unit Cell and Crystal Structure of Nordstrandite, Al(OH)₃. *Acta Crystallogr. Sect. B Struct. Crystallogr. Cryst. Chem.* **1970**, *26*, 649–652.
- (8) Clark, G. R.; Rodgers, K. A.; Henderson, G. S. The Crystal Chemistry of Doyleite, Al(OH)₃. *Z. Kristallogr. N. Cryst. Struct.* **1998**, *213*, 96–100.
- (9) Britto, S.; Kamath, P. V. Polytypism in the Lithium-Aluminum Layered Double Hydroxides: The [LiAl₂(OH)₆]⁺ Layer as a Structural Synthon. *Inorg. Chem.* **2011**, *50*, S619–S627.
- (10) Smith, D. W. Ionic Hydration Enthalpies - Journal of Chemical Education (ACS Publications and Division of Chemical Education). *J. Chem. Educ.* **1977**, *54*, 540–542.
- (11) Pachayappan, L.; Kamath, P. V. Effect of Hydration on Polytypism and Disorder in the Sulfate-Intercalated Layered Double Hydroxides of Li and Al. *Clays Clay Miner.* **2019**, *67*, 154–162.
- (12) Saalfeld, M.; Wedde, M. Refinement of the Crystal Structure of Gibbsite, Al(OH)₃ Introduction of Gibbsite (Hydrargillite), Al(OH)₃, Is a Sheet Structure Crystallizing Usually in Pseudohexagonal Platelets or Prisms with Monoclinic Symmetry. Occasionally It May Also Cr. *Z. Kristallogr. N. Cryst. Struct.* **1974**, *139*, 129–135.
- (13) Nagendran, S.; Periyasamy, G.; Kamath, P. V. Structure Models for the Hydrated and Dehydrated Nitrate-Intercalated Layered Double Hydroxide of Li and Al. *Dalton Trans.* **2016**, *45*, 18324–18332.
- (14) Nagendran, S.; Kamath, P. V. Structure of the Chloride- and Bromide-Intercalated Layered Double Hydroxides of Li and Al - Interplay of Coulombic and Hydrogen-Bonding Interactions in the Interlayer Gallery. *Eur. J. Inorg. Chem.* **2013**, *2013*, 4686–4693.
- (15) Pachayappan, L.; Kamath, P. V. Effect of Hydration on Polytypism and Disorder in the Sulfate-Intercalated Layered Double Hydroxides of Li and Al. *Clays Clay Miner.* **2019**, *67*, 154–162.
- (16) Pachayappan, L.; Kamath, P. V. Reversible Hydration of the Perchlorate-Intercalated Layered Double Hydroxides of Li and Al: Structure Models for the Dehydrated Phases. *Bull. Mater. Sci.* **2020**, *43*, 1.
- (17) Britto, S.; Kamath, P. V. Structure of Bayerite-Based Lithium - Aluminum Layered Double Hydroxides (LDHs) : Observation of Monoclinic Symmetry. *Inorg. Chem.* **2009**, *48*, 11646–11654.
- (18) Nagendran, S.; Periyasamy, G.; Kamath, P. V. Hydration-Induced Interpolytype Transformations in the Bayerite-Derived

Nitrate-Intercalated Layered Double Hydroxide of Li and Al. *J. Solid State Chem.* **2018**, *266*, 226–232.

(19) Nagendran, S.; Periyasamy, G.; Kamath, P. V. DFT Study of Polymorphism in Al(OH)₃: A Structural Synthon Approach. *Z. Anorg. Allg. Chem.* **2015**, *641*, 2396–2403.

(20) Venkataraman, K.; Pachayappan, L. Synthesis of Nordstrandite and Nordstrandite-Derived Layered Double Hydroxides of Li and Al: A Comparative Study with the Bayerite Counterpart. *Z. Anorg. Allg. Chem.* **2020**, *646*, 1916–1921.

(21) Łasocha, W.; Lewinski, K. PROSZKI – a System of Programs for Powder Diffraction Data Analysis. *J. Appl. Crystallogr.* **1994**, *27*, 437–438.

(22) Treacy, M. M. J.; Newsam, J. M.; Deem, M. W. A general recursion method for calculating diffracted intensities from crystals containing planar faults. *Proc. R. Soc. A* **1991**, *433*, 499.

(23) Treacy, M. M. J.; Deem, M. W.; Newsam, J. M. *DIFFaX*, version 1.812. 2005.

(24) Nagendran, S.; Kamath, P. V. Synthon Approach to Structure Models for the Bayerite-Derived Layered Double Hydroxides of Li and Al. *Inorg. Chem.* **2017**, *56*, 5026–5033.

(25) Favre-Nicolin, V.; Cerný, R. “Free Objects for Crystallography”: A Modular Approach to Ab Initio Structure Determination from Powder Diffraction. *J. Appl. Crystallogr.* **2002**, *35*, 734–743.

(26) Rodríguez-Carvajal, J. A.. FULLPROF: A Program for Rietveld Refinement and Pattern Matching Analysis. *Abstracts of the Satellite Meeting on Powder Diffraction of the XVth Congress of the International Union of Crystallography*; Toulouse: France, 1990; p 127.

(27) Larson, A. C.; Von Dreele, R. B. *General Structure Analysis System (GSAS)*; Los Alamos National Laboratory Report LAUR, 2004; Vol. 748, pp 86–748.

(28) Britto, S.; Kamath, P. V. Structural Synthon Approach to the Study of Stacking Faults in the Layered Double Hydroxides of Lithium and Aluminum. *Z. Anorg. Allg. Chem.* **2012**, *638*, 362–365.

(29) Pachayappan, L.; Nagendran, S.; Kamath, P. V. Polytypism in Alumite-like Layered Double Hydroxides of M (Zn²⁺, Ni²⁺) and Al: A Structural Transformation from Monoclinic to Orthorhombic Symmetry. *Cryst. Growth Des.* **2020**, *20*, 3264–3271.

(30) Narayanappa, A. N.; Nagendran, S.; Kamath, P. V. Synthesis, Polytypism, and Dehydration Behaviour of Nitrate-Intercalated Layered Double Hydroxides of Ca and Al. *New J. Chem.* **2021**, *45*, 5837–5844.

(31) Benco, L.; Tunega, D.; Hafner, J.; Lischka, H. Upper Limit of the O–H···O Hydrogen Bond. Ab Initio Study of the Kaolinite Structure. *J. Phys. Chem. B* **2001**, *105*, 10812–10817.

(32) Taichi, S. Preparation of Aluminum Hydride. *J. Jpn. Inst. Light Metals* **1988**, *38*, 731–739.